Gastric Cancer (2019) 22:314–322
https://doi.org/10.1007/s10120-018-0862-6

ORIGINAL ARTICLE

# Solid-type poorly differentiated adenocarcinoma of the stomach: clinicopathological and molecular characteristics and histogenesis

Tomio Arai[1] · Yoko Matsuda[1] · Junko Aida[2] · Kaiyo Takubo[2] · Toshiyuki Ishiwata[2]

Received: 16 May 2018 / Accepted: 30 July 2018 / Published online: 7 August 2018


## Abstract

**Background** Despite predominant microsatellite instability (MSI) in intestinal-type gastric carcinomas, we found the most frequent MSI in solid-type poorly differentiated adenocarcinoma (PDA). Although this tumor is classified as PDA, it is hypothesized to possess peculiar features among PDAs. The present study aimed to clarify the clinicopathological and molecular characteristics of this tumor.

**Methods** We examined the expression of p53, mismatch-repair proteins, and mucin core glycoproteins; microsatellite status; and mutations in *KRAS* and *BRAF*, as well as clinicopathological features, in 54 cases of PDA of the stomach (31 solid-type PDAs and 23 non-solid-type PDAs).

**Results** The proportion (51.6%) of MSI in solid-type PDA was significantly higher than that in non-solid-type PDA (4.5%) ($p = 0.00022$). The proportion of absent expression of MLH1 (58.1%) and PMS2 (51.6%) in solid-type PDA was significantly higher than that in non-solid-type PDA (4.5 and 8%) ($p < 0.0001$). No differences were found in the mutations of *KRAS* and *BRAF* among PDAs. MSI-positive solid-type PDA was significantly associated with older age, female predominance, lower third location, concordant glandular component, and absent MLH1 and PMS2 expression.

**Conclusions** These results suggest that MSI-positive solid-type PDA has peculiar clinicopathological features and that MSI with absent MLH1 and PMS2 expression may play an important role in tumor development. In addition, from the viewpoint of histogenesis, MSI-positive solid-type PDA may originate from differentiated-type adenocarcinoma.

**Keywords** Microsatellite instability · Poorly differentiated adenocarcinoma · Solid carcinoma · Elderly · Stomach

## Introduction

Adenocarcinoma with little glandular formation is generally diagnosed as poorly differentiated adenocarcinoma (PDA). In gastric cancer, it is well known that PDAs include tumors showing various morphologies such as poorly cohesive adenocarcinoma, signet-ring cell carcinoma, and so on [1, 2]. Although solid adenocarcinoma was classified as a poorly differentiated variant of tubular adenocarcinoma [1, 3–5], this tumor, along with carcinoma with lymphoid stroma, medullary carcinoma with lymphoid stroma, and lymphoepithelioma-like carcinoma, usually tends to be diagnosed as PDA in daily practice because of little glandular structure. Consequently, PDAs are not a single entity, but constitute diverse diseases.

On the other hand, according to the Japanese Classification of Gastric Cancer [2], PDAs are subdivided into two groups according to the morphology of tumor nests: solid type and non-solid type because of the existence of PDAs with better prognosis. The evidence that solid-type PDAs show different biological behaviors from non-solid-type PDA resulted in this subclassification [6]. Our previous study demonstrated a close relationship between microsatellite instability (MSI) and solid-type histology [7]. In addition, it is controversial whether solid-type PDA or solid carcinoma is classified as diffuse type in Laurén's classification [8] or as undifferentiated type in

**Electronic supplementary material** The online version of this article (https://doi.org/10.1007/s10120-018-0862-6) contains supplementary material, which is available to authorized users.

✉ Tomio Arai
arai@tmig.or.jp

[1] Department of Pathology, Tokyo Metropolitan Geriatric Hospital, 35-2 Sakaecho, Itabashi-ku, Tokyo 173-0015, Japan

[2] Research Team for Geriatric Pathology, Tokyo Metropolitan Institute of Gerontology, Tokyo, Japan

Sugano–Nakamura's classification [9]. Thus, morphology, MSI, and biological behavior in solid-type PDA are different from those in non-solid-type PDAs. There have only been a few pathological reports until now, and the details regarding solid-type PDA of the stomach remain obscure [4, 10–14].

We hypothesized that solid-type PDA has distinct features in comparison with non-solid-type PDA. The present study aimed to clarify the clinicopathological and molecular features of solid-type PDA as well as its histogenesis.

## Materials and methods

### Patients

We selected 54 patients with poorly differentiated gastric carcinomas (31 solid-type PDAs and 23 non-solid-type PDAs) from cases surgically treated at Tokyo Metropolitan Geriatric Hospital between 2000 and 2007, without neoadjuvant therapy. They comprised 31 men and 23 women, with a median age of 77 years, ranging from 56 to 99 years. Patients with Lynch syndrome were excluded.

### Histopathological evaluation

All tissue samples were fixed in 15% formalin after resection and then embedded in paraffin using standard procedures. Serial sections of 3 and 10 μm thickness were prepared from each specimen. The 3-μm-thick sections were used for hematoxylin–eosin and elastica van Gieson staining, immunostaining, and in situ hybridization, whereas the 10-μm-thick sections were used for DNA extraction.

Fifty-four cases of PDA were pathologically diagnosed according to the Japanese Classification of Gastric Carcinoma as solid-type PDA and non-solid-type PDA [2]. Briefly, solid-type PDA comprises cancer cells that have formed a solid or sheet-like structure and exhibit expansive growth. Non-solid-type PDA is composed of cancer cells with small glands, in small clusters or a trabecular structure, or is composed of isolated cancer cells and frequently exhibits infiltrative growth. The growth pattern, depth of invasion, location, concordant glandular component, Crohn's-like lymphoid reaction, and tumor-infiltrating lymphocytes were estimated as described previously [15, 16]. Because of histological similarity with solid-type PDA, neuroendocrine cell carcinoma, malignant lymphoma, and malignant melanoma were excluded histopathologically. Venous and lymphatic permeations were evaluated histologically using hematoxylin–eosin- and elastica van Gieson-stained slides.

### Immunohistochemical analysis of p53 and mismatch repair and mucin core proteins

Expression of p53, mismatch-repair proteins, and mucin core glycoproteins was evaluated by immunohistochemistry. Endogenous peroxidase was blocked by treatment with 0.3% $H_2O_2$ in methanol for 15 min. The sections for p53 and mismatch-repair proteins were heated at 100 °C for 10 min for antigen retrieval. The slides were immunostained by the streptavidin–biotin method using an anti-p53 antibody (MO-7, dilution 1:100, Nichirei, Tokyo, Japan) and anti-human MLH1 (clone G168-15, dilution 1:100, BD Pharmingen, Tokyo, Japan), MSH2 (clone FE11, dilution 1:100, Calbiochem, Billerica, MA, USA), MSH6 (clone EP49, dilution 1:50, Dako, Glostrup, Denmark), and PMS2 (clone A16-4, dilution 1:50, BD Pharmingen) monoclonal antibodies, and developed with a diaminobenzidine substrate. Hematoxylin was used for counterstaining. For mismatch-repair proteins, adjacent normal tissues were used as internal controls. The intensity of nuclear staining in the entire tumor was classified as negative, weak, or positive. Focal or heterogeneous staining patterns were recorded. For the statistical analysis, weak staining was considered as negative for mismatch-repair proteins, and p53 expression was classified based on the presence or the absence of overexpression.

To determine the mucin phenotype, slides were stained with anti-Muc-2 glycoprotein (clone Ccp58, dilution 1:50, Novocastra Laboratories, Newcastle upon Tyne, UK), Muc-5AC (clone CLH2, dilution 1:500, Leica Biosystems, Newcastle Upon Tyne, UK), Muc-6 (cline NCL-MUC6, dilution 1:20, Novocastra Laboratories), and CD10 (clone 56C6, ready to use, Nichirei, Tokyo) antibodies followed by counterstaining with hematoxylin. The mucin phenotypes were classified into four groups: gastric type, intestinal type, mixed type, and unclassified type based on the positivity of each mucin phenotype, as described previously by other investigators [17].

### In situ hybridization of Epstein–Barr virus-encoded small RNA (EBER)

To detect Epstein–Barr virus (EBV) infection, 3-μm-thick sections were stained using in situ hybridization (Dako, Tokyo, Japan) according to the manufacturer's instruction.

### DNA extraction

One 10-μm section on glass slides was used for DNA extraction. After deparaffinization, the tumor tissues were scraped from the semi-dried section with a blade under a stereomicroscope. DNA was extracted separately from the tumor

and normal areas. The samples were incubated overnight at 56 °C in lysis buffer, and DNA was extracted from all samples using a phenol–chloroform procedure described previously [7].

### Detection of *KRAS* and *BRAF* mutations

Mutations in *KRAS* codon 12 and 13 and *BRAF* (V600E) were examined using polymerase chain reaction–restriction fragment length polymorphism (PCR–RFLP). The primer sequences and PCR conditions have been described by other investigators [18, 19].

### Microsatellite analysis

Microsatellite status was examined using five markers consisting of two mononucleotide markers (*BAT25* and *BAT26*) and three dinucleotide markers (*D3S1067, D5S346*, and *D18S58*). The primer sequences and PCR conditions are published elsewhere [20]. The PCR products were mixed with an equal volume of loading buffer (95% formamide, 0.05% bromophenol blue, and 0.5 mol/L EDTA), electrophoresed on denaturing 6% polyacrylamide gels at 50 °C, and stained with a silver staining kit (Atto, Tokyo, Japan) according to the manufacturer's instruction. Additional peaks at a microsatellite locus in the tumor DNA compared with normal DNA from the same patient were interpreted as MSI. Cases with MSI in 2 or more loci were interpreted as exhibiting high MSI (MSI-H), cases with MSI in only one locus were called low MSI (MSI-L), and cases that did not show MSI in any of the five markers of the microsatellite panels were called microsatellite stable (MSS).

### Statistical analysis

All data were subjected to statistical analysis using SPSS version 22 (IBM). Comparisons among continuous and categorical variables were made using the Mann–Whitney test, Chi-square test, or Fisher's exact probability test. *P* values of less than 0.05 (two-sided) indicated significance.

**Table 1** Clinicopathologic characteristics of poorly differentiated gastric cancer

| | Solid-type PDA[a] ($n=31$) | Non-solid-type PDA[a] ($n=23$) | *p* value |
|---|---|---|---|
| Age (years; median, range) | 78 (66–99) | 74 (56–89) | 0.56[b] |
| Sex | | | |
| Male | 18 (58.1) | 13 (56.5) | 0.91 |
| Female | 13 (41.9) | 10 (43.5) | |
| Location | | | |
| Upper | 2 (6.5) | 7 (30.4) | 0.0067 |
| Middle | 8 (25.8) | 8 (34.8) | |
| Lower | 21 (67.7) | 6 (26.1) | |
| Diffuse | 0 (0) | 2 (8.7) | |
| Tumor size (mm; median, range) | 85 (35–190) | 90 (20–185) | 0.99[b] |
| Depth of invasion | | | |
| pT1 | 1 (3.2) | 2 (8.7) | 0.36 |
| pT2 | 4 (12.9) | 1 (4.3) | |
| pT3 | 3 (9.7) | 5 (21.7) | |
| pT4 | 23 (74.2) | 15 (65.2) | |
| Lymphatic invasion | | | |
| Present | 30 (96.8) | 21 (91.3) | 0.39 |
| Absent | 1 (3.2) | 2 (8.7) | |
| Venous invasion | | | |
| Present | 28 (90.3) | 21 (91.3) | 0.90 |
| Absent | 3 (9.7) | 2 (8.7) | |
| Lymph node metastasis | | | |
| pN0 | 10 (32.3) | 4 (17.4) | 0.22 |
| pN1–3 | 21 (67.7) | 19 (82.6) | |

The data were analyzed using $\chi^2$ test except for those of the age and tumor size

[a]*PDA* poorly differentiated adenocarcinoma

[b]The age and tumor size between solid-type and non-solid-type PDAs were statistically analyzed using Mann–Whitney test

## Results

### Clinicopathological findings

The clinicopathological characteristics of each PDA subtype are summarized in Table 1. Solid-type PDA predominantly occurred in the lower third location ($p=0.007$). In other features, there were no significant differences between the two groups.

### Histopathology of solid-type PDA

Histologically, solid-type PDA showed expansive growth with a scattered Crohn's-like lymphoid reaction around the tumor (Fig. 1a). The tumor cells in solid-type PDA had oval vesicular nuclei with prominent nucleoli and

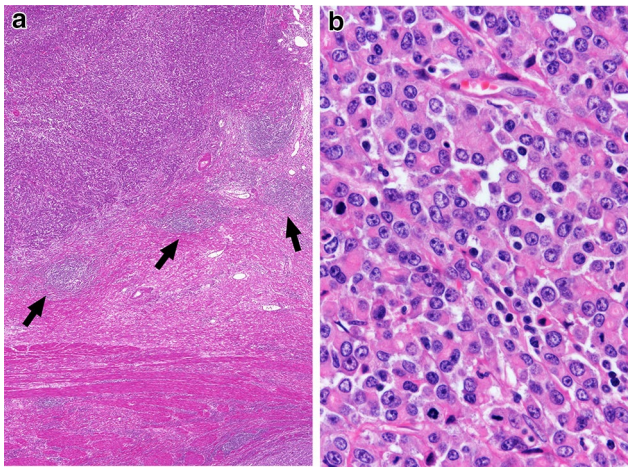


**Fig. 1** Histopathological findings of solid-type PDA of the stomach. **a** Tumor grows expansively with scattered Crohn's-like lymphoid reactions (arrows) in the gastric wall. Hematoxylin–eosin staining. **b** Tumor cells show oval vesicular nuclei with prominent nucleoli and abundant eosinophilic cytoplasm. The tumor forms a solid nest with numerous tumor-infiltrating lymphocytes. Hematoxylin–eosin staining

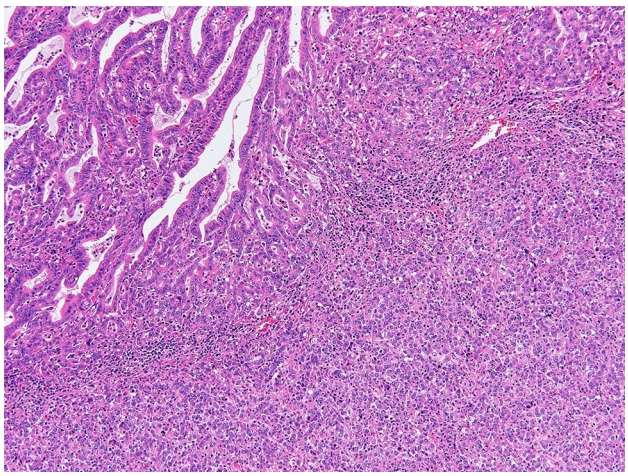

**Fig. 2** Histology of solid-type PDA co-existent with a glandular adenocarcinoma component. Solid-type PDA are predominantly present at the invasive area (right lower area) with glandular adenocarcinoma coexistence at the mucosal area. Hematoxylin–eosin staining

abundant eosinophilic cytoplasm (Fig. 1b), forming a solid nest with scanty stroma. Tumor-infiltrating lymphocytes were scattered within the tumor. Solid-type PDA frequently had a glandular adenocarcinoma component at the mucosal or peripheral area (Fig. 2), and showed prominent lymphatic and venous invasion.

**Table 2** Results of immunohistochemistry and in situ hybridization

| | Solid-type PDA[a] ($n=31$) | Non-solid-type PDA[a] ($n=23$) | $p$ value |
|---|---|---|---|
| MLH1 | | | |
| Positive | 13 (41.9) | 22 (95.7) | < 0.0001 |
| Negative | 18 (58.1) | 1 (4.3) | |
| MSH2 | | | |
| Positive | 31 (100) | 23 (100) | NS[a] |
| Negative | 0 (0) | 0 (0) | |
| MSH6 | | | |
| Positive | 31 (100) | 23 (100) | NS[a] |
| Negative | 0 (0) | 0 (0) | |
| PMS2 | | | |
| Positive | 16 (51.6) | 21 (91.3) | 0.0019 |
| Negative | 15 (48.4) | 2 (8.7) | |
| p53 overexpression | | | |
| Present | 12 (38.7) | 14 (60.9) | 0.064 |
| Absent | 19 (61.3) | 9 (39.1) | |
| Mucin phenotype | | | |
| Gastric type | 7 (22.6) | 7 (30.4) | 0.57 |
| Intestinal type | 7 (22.6) | 4 (17.4) | |
| Mixed type | 6 (19.3) | 7 (30.4) | |
| Unclassified type | 11 (35.5) | 5 (21.7) | |
| EBER | | | |
| Positive | 2 (6.5) | 0 (0) | 0.21 |
| Negative | 29 (93.5) | 23 (100) | |

The data represent the number of cases with percentage in the parentheses. The data were analyzed using $\chi^2$ test

[a]*PDA* poorly differentiated adenocarcinoma, *NS* not significant

## Immunohistochemistry and in situ hybridization of EBER

The results of the immunohistochemical analysis are summarized in Table 2. When PDA had a concordant glandular component, expression pattern of each protein in PDA was the same as that in concordant glandular component. The proportion of absent expression of MLH1 (58.1%) and PMS2 (51.6%) in solid-type PDA was significantly higher than that in non-solid-type PDA (4.3 and 8.7%, respectively; $p < 0.0001$). Representative immunohistochemical features of solid-type PDA are shown in Fig. 3. There were no differences in the expression of other proteins between the two subtypes of PDA. Although there were no significant differences in the mucin phenotype, the proportion (35.5%) of the unclassified type tended to be higher in solid-type PDA than that (21.7%) in non-solid-type PDA. A positive reaction for EBER was found in only 2 cases (2.6%) out of 54 PDAs. Both cases showed solid-type histology and were located in the middle-third region of the stomach.

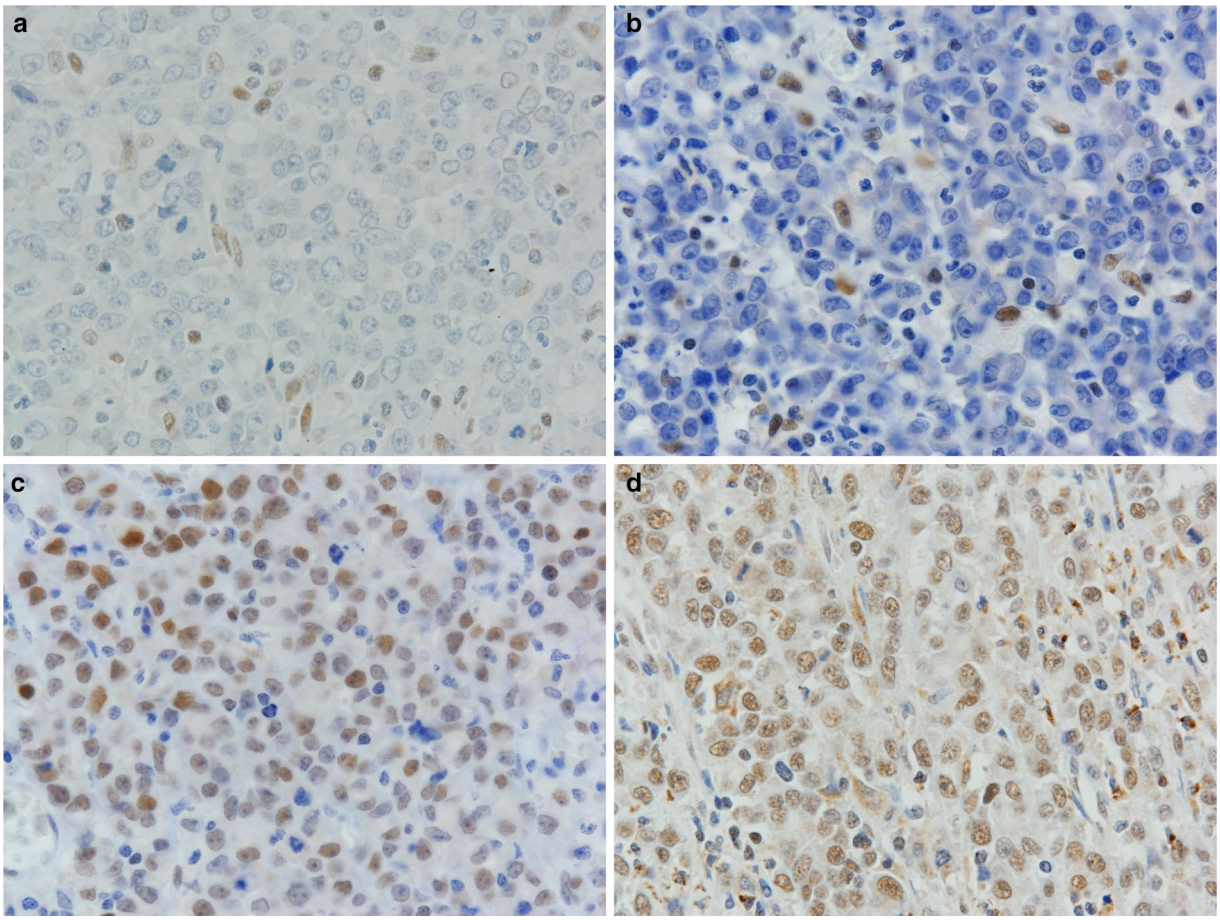


**Fig. 3** Immunohistochemical findings of MSI-positive solid-type PDA. MSI-positive solid-type PDA showing the absence of MLH1 (**a**) and PMS2 (**b**) expression, although tumor-infiltrating lymphocytes, fibroblasts, and endothelial cells show a positive reaction. Both MSH2 (**c**) and MSH6 (**d**) showed a positive reaction in the nuclei of tumor cells. Counterstaining, hematoxylin

**Table 3** Results of molecular findings

| | Solid-type PDA[a] ($n=31$) | Non-solid-type PDA[a] ($n=23$) | $p$ value[b] |
|---|---|---|---|
| Microsatellite status | | | |
| MSI[a] | 16 (51.6) | 1 (4.3) | 0.00022 |
| MSS[a] | 15 (48.4) | 22 (95.7) | |
| *KRAS* (codon 12 and 13) | | | |
| Wild type | 26 (83.9) | 21 (91.3) | 0.42 |
| Mutant type | 5 (16.1) | 2 (8.7) | |
| *BRAF* (V600) | | | |
| Wild type | 30 (96.8) | 22 (95.7) | 0.83 |
| Mutant type | 1 (3.2) | 1 (4.3) | |

The data represent the number of cases with percentage in the parentheses

[a]*PDA* poorly differentiated adenocarcinoma, *MSI* microsatellite unstable, *MSS* microsatellite stable

[b]The data were analyzed using $\chi^2$ test

## Molecular pathology findings

Among 54 gastric PDAs, MSI was observed in 17 cases (31.5%). All cases demonstrated MSI-H. The proportion of MSI in solid-type PDA (16/31, 51.6%) was significantly higher than that in non-solid-type PDA (1/23, 4.3%) (Table 3, $p=0.00022$).

No differences were observed in the mutations of *KRAS* and *BRAF* among gastric PDAs, but solid-type PDA showed a higher proportion of *KRAS* (16.1%) and *BRAF* (3.2%) mutations than non-solid-type PDA.

## Clinicopathological characteristics of microsatellite-unstable solid-type PDAs

Microsatellite-unstable solid-type PDA was significantly related with female predominance, lower third location, tumor-infiltrating lymphocytes, Crohn's-like lymphoid reaction, a concordant glandular component, absent MLH1 and PMS2 expression, and less frequent p53 overexpression

**Table 4** Comparison between microsatellite-unstable and stable solid-type poorly differentiated adenocarcinoma

| Clinicopathological valuables | MSI[a] ($n=16$) | MSS[a] ($n=15$) | $p$ value |
|---|---|---|---|
| Age (years; median, range) | 80 (69–99) | 75 (66–84) | 0.081[b] |
| Gender (male/female) | 6/10 | 12/3 | 0.017 |
| Location (upper/middle/lower) | 0/0/16 | 2/8/5 | <0.001 |
| Tumor size (mm; median, range) | 86.5 (37–190) | 80 (35–130) | 0.28 |
| Growth pattern (expansive/infiltrating/mixed) | 14/1/1 | 7/5/3 | 0.050 |
| Tumor-infiltrating lymphocyte (+/−) | 15/1 | 7/8 | 0.0039 |
| Crohn's-like lymphoid reaction (+/−) | 15/1 | 9/6 | 0.025 |
| Concordant glandular component (+/−) | 13/3 | 6/9 | 0.018 |
| Venous permeation (+/−) | 13/3 | 15/0 | 0.078 |
| Lymphatic invasion (+/−) | 16/0 | 14/1 | 0.29 |
| Lymph node metastasis (+/−) | 10/6 | 11/4 | 0.52 |
| MLH1 expression (+/−) | 1/15 | 12/3 | <0.0001 |
| MSH2 expression (+/−) | 16/0 | 15/0 | NS[a] |
| MSH6 expression (+/−) | 16/0 | 15/0 | NS[a] |
| PMS2 expression (+/−) | 1/15 | 15/0 | <0.0001 |
| p53 overexpression (+/−) | 3/13 | 9/6 | 0.018 |
| Mucin phenotype (gastric/intestinal/mixed/unclassified) | 5/3/5/3 | 2/4/1/8 | 0.096 |

The data represent the number of cases. The data were analyzed using $\chi^2$ test except for the age and tumor size

[a]*MSI* microsatellite unstable, *MSS* microsatellite stable, *NS* not significant

[b]The age and tumor size in each group were analyzed using Mann–Whitney test

(Table 4). Regarding age and growth pattern, microsatellite-unstable solid-type PDA tended to relate to older age and an expansive growth pattern than microsatellite-stable solid-type PDA.

### Relationship between the microsatellite status and concordant glandular component in solid-type PDA

Solid-type PDA had a frequently concordant glandular component in its mucosal or peripheral region. Compared with solid-type PDA without a glandular component, solid-type PDA with a concordant glandular component was significantly associated with MSI ($p=0.019$).

## Discussion

We showed that approximately half of solid-type PDAs have peculiar clinicopathological features such as older age, female predominance, antral location, prominent tumor-infiltrating lymphocytes, Crohn's-like lymphoid reaction, and a concordant glandular component. In addition, solid-type PDA with MSI, probably derived from glandular adenocarcinoma, was closely correlated with absent MLH1 expression and lower p53 expression.

The present study demonstrates the clinicopathological characteristics of solid-type PDA in comparison with non-solid-type PDA. These features were reflected from those of microsatellite-unstable solid-type PDA. Notably, MSI-positive PDA was limited to occur in the gastric antrum. The tumor shared pathological and biological features with those occurring in patients with medullary carcinoma of the colon, i.e., vesicular nuclei with eosinophilic cytoplasm, tumor-infiltrating lymphocytes, Crohn's-like lymphoid reaction, and a concordant glandular component [21]. Although gastric solid-type carcinoma could be considered as a gastric counterpart of colonic medullary carcinoma due to similar phenotype, their carcinogenesis is considered to be partly different because of lower *BRAF* mutation in gastric solid-type PDA. In accordance with our results, Choi et al. demonstrated that MSI-positive gastric cancers show prominent vessel invasion [22]. However, their report, together with our data, indicated a relatively lower incidence of node metastasis than that in non-solid-type PDA. Thus, it is suggested that solid-type carcinoma is a peculiar tumor among PDAs.

The present study showed that the clinicopathological and molecular features of solid-type PDA differ from those of non-solid-type PDA. In fact, solid-type PDA shares histological morphology features such as few glandular formations with non-solid-type PDA. However, several studies have shown that solid-type PDA exhibits different clinicopathological features in comparison with non-solid-type PDA [4, 11–13, 23]. Since the 12th version of the Japanese Classification of Gastric Cancer, PDA has been subclassified

into two groups: solid-type and non-solid-type [24]. At that time, the prognosis of solid-type PDA was considered better than that of non-solid-type PDA [6]. Subsequently, research advances revealed that solid-type PDA has a relatively good prognosis. On the other hand, it is likely that solid-type PDA in the Japanese classification is equivalent to solid carcinoma in the WHO classification [1], which is described as a poorly differentiated variant of tubular adenocarcinoma. In addition, from the viewpoint of molecular pathology, the alteration patterns in "solid adenocarcinoma" were similar to those of intestinal-type gastric cancer [25]. Thus, solid-type PDA should be distinguished from non-solid-type PDA.

This study provides data that approximately half of solid-type PDA showed MSI. In sporadic gastric cancer, MSI is induced by hypermethylation of the *MLH1* gene promoter [26]. The proportion of MSI in gastric cancer increases with advancing age, reaching more than 35% in elderly women aged 85 years or older [7, 26]. Thus, MSI with absent MLH1 expression may play an important role in tumor development. In addition, despite numerous reports indicating a significant relationship between intestinal-type histology and MSI [27], our previous study clearly showed that solid-type PDA was one of the most frequent MSI in gastric cancer as well as papillary adenocarcinoma [7]. MSI-positive cancer could be targeted by immune checkpoint blockade with pembrolizumab and so on, whereas solid-type PDA is uncommon in younger patients, but accounts for approximately 20% in elderly patients [28]. Thus, from the viewpoint of treatment and demographic dynamics, it is expected that the incidence of this type of cancer will increase in the near future.

In the present study, the proportions of *KRAS* (14.1%) and *BRAF* (3.8%) mutations in solid-type PDA were higher than those (4.2 and 0.14%, respectively) reported previously in GCs [29]. van Grieken et al. demonstrated a close relationship between *KRAS* mutation and MSI in GCs [29]. Consequently, *KRAS* mutation is expected to be more frequent in solid-type PDA than in other histological types. On the other hand, Jiao et al. reported that the pattern of genetic alteration in solid carcinoma was similar to that in tubular adenocarcinoma [25]. Thus, solid-type PDA may have a specific genetic profile.

The present study demonstrated that MSI-positive solid-type PDA shares clinicopathological features with Epstein–Barr virus (EBV)-associated GCs (EBVaGC) such as poorly differentiated adenocarcinoma with prominent lymphocyte infiltration. Moreover, from the molecular viewpoint, reports by other investigators also showed the two tumors shared a CpG mutator phenotype (CIMP) and microsatellite instability [30]. However, EBVaGC shows clinicopathological characteristics such as male predominance, proximal location, and lymphoepithelioma-like histology [31], whereas MSI-positive solid-type GC demonstrated female predominance, antral location, and PDA with tumor-infiltrating lymphocytes. Thus, these results suggest that MSI-positive solid-type PDA demonstrates an entity different from EBVaGC.

As for the histogenesis of solid-type PDA with MSI, the tumor frequently had a concordant glandular component in its mucosal and/or peripheral area. Most early GCs with MSI showed a glandular histology, and a poorly differentiated component appeared with cancer progression. MSI-positive solid-type PDA showed a concordant glandular component more frequently [7]. The histological features together with molecular findings, suggest that MSI-positive solid-type carcinoma originates from glandular carcinoma. Therefore, we propose a histogenesis of MSI-positive solid-type PDA. MSI-positive solid-type carcinoma principally develops as glandular adenocarcinoma including tubular and papillary adenocarcinoma, and then progresses to a more poorly differentiated one, especially in an invasive region. A small amount of glandular component might remain in the peripheral or superficial region of the tumor.

Diagnosing MSI-positive solid-type PDA is important in daily practice. Recent advances in molecular biology have demonstrated the comprehensive molecular characterization of GC [32]. GCs are classified into four types: EBV-related, CIMP-positive type; microsatellite instability, hypermutated type; genomically stable type; and chromosomal instability type. As approximately half of the solid-type PDAs could belong to the microsatellite instability, hypermutated type, this tumor type could be targeted using molecular targeted agents [33, 34]. Thus, pathologists should make a correct diagnosis for GC with MSI. Solid-type PDA is a representative tumor with MSI in GCs. Although molecular pathological examination using microsatellite instability is not available in most pathology departments, immunohistochemistry of mismatch-repair proteins is useful for the correct diagnosis of solid-type PDA with MSI.

The present study has several limitations. First, the sample was biased towards the elderly. That was why the proportion of EBVaGC in this study was lower than expected. Second, the biological behavior of MSI-positive PDA was not adequately examined because of insufficient follow-up observation. Third, to more reliably distinguish MSI-positive PDA from other types of GC, genetic alterations should be examined in further detail.

In conclusion, we have shown that MSI-positive solid-type PDA has peculiar clinicopathological features and that MSI with absent MLH1 expression may play an important role in tumor development. In addition, from the viewpoint of histogenesis, MSI-positive solid-type PDA may originate from differentiated-type adenocarcinoma.

**Acknowledgements** The authors thank the staff at the Department of Pathology, Tokyo Metropolitan Geriatric Hospital, and Mr. Shunsuke

Kanari for providing technical assistance. This study was supported in part by the JSPS KAKENHI Grant Numbers JP25460428, JP16K08664 and AMED under Grant Number JP18kk0205004 (to T.A.).

## Compliance with ethical standards

**Conflict of interest** The authors have disclosed that they have no significant relationships with, or financial interest in, any commercial companies pertaining to this article.

**Research involving human participants** This study was approved by the Ethics Committee of Tokyo Metropolitan Geriatric Hospital (#230225, R16-23).

## References


1. Lauwers GY, Carneiro F, Graham DY, Curado MP, Franceschi S, Montgomery E, et al. Gastric carcinoma. In: Bosman FT, Carneiro F, Hruban RH, Theise ND, editors. WHO classification of tumours of the digestive system, 4th ed. Lyon: WHO Publisher, 2010. p. 48–63.
2. Japanese Gastric Cancer Assocation. Japanese classification of gastric carcinoma: 3rd English edition. Gastric Cancer. 2011;14:101–12.
3. Watanabe H, Enjoji M, Imai T. Gastric carcinoma with lymphoid stroma. Its morphologic characteristics and prognostic correlations. Cancer. 1976;38:232–43.
4. Minamoto T, Mai M, Watanabe K, Ooi A, Kitamura T, Takahashi Y, et al. Medullary carcinoma with lymphocytic infiltration of the stomach. Clinicopathologic study of 27 cases and immunohistochemical analysis of the subpopulations of infiltrating lymphocytes in the tumor. Cancer. 1990;66:945–52.
5. Wang HH, Wu MS, Shun CT, Wang HP, Lin CC, Lin JT. Lymphoepithelioma-like carcinoma of the stomach: a subset of gastric carcinoma with distinct clinicopathological features and high prevalence of Epstein–Barr virus infection. Hepatogastroenterology. 1999;46:1214–9.
6. Koda K, Kino I. Histopathological classification of poorly differentiated adenocarcinoma of the stomach into solid and non-solid types. Stomach Intestine. 1991;26:1167–72 **(in Japanese with English abstract)**.
7. Arai T, Sakurai U, Sawabe M, Honma N, Aida J, Ushio Y, et al. Frequent microsatellite instability in papillary and solid-type, poorly differentiated adenocarcinomas of the stomach. Gastric Cancer. 2013;16:505–12.
8. Laurén P. The Two histological main types of gastric carcinoma: diffuse and so-called intestinal-type carcinoma. An attempt at a histo-clinical classification. Acta Pathol Microbiol Scand. 1965;64:31–49.
9. Sugano H, Nakamura K, Kato Y. Pathological studies of human gastric cancer. Acta Pathol Jpn. 1982;32(Suppl 2):329–47.
10. Adachi Y, Mori M, Maehara Y, Sugimachi K. Poorly differentiated medullary carcinoma of the stomach. Cancer. 1992;70:1462–6.
11. Ueyama T, Tsuneyoshi M. Poorly differentiated solid type adenocarcinomas in the stomach: a clinicopathologic study of 71 cases. J Surg Oncol. 1992;51:81–7 **(discussion 7–8)**.
12. Yokota T, Kunii Y, Saito T, Teshima S, Yamada Y, Takahashi M, et al. Poorly differentiated, solid-type adenocarcinoma of the stomach. Ups J Med Sci. 1999;104:207–16.
13. Lu BJ, Lai M, Cheng L, Xu JY, Huang Q. Gastric medullary carcinoma, a distinct entity associated with microsatellite instability-H, prominent intraepithelial lymphocytes and improved prognosis. Histopathology. 2004;45:485–92.
14. Hirai H, Yoshizawa T, Morohashi S, Haga T, Wu Y, Ota R, et al. Clinicopathological significance of gastric poorly differentiated medullary carcinoma. Biomed Res. 2016;37:77–84.
15. Graham DM, Appelman HD. Crohn's-like lymphoid reaction and colorectal carcinoma: a potential histologic prognosticator. Mod Pathol. 1990;3:332–5.
16. Naito Y, Saito K, Shiiba K, Ohuchi A, Saigenji K, Nagura H, et al. $CD8^+$ T cells infiltrated within cancer cell nests as a prognostic factor in human colorectal cancer. Cancer Res. 1998;58:3491–4.
17. Sugai T, Habano W, Uesugi N, Jao YF, Nakamura S, Abe K, et al. Three independent genetic profiles based on mucin expression in early differentiated-type gastric cancers—a new concept of genetic carcinogenesis of early differentiated-type adenocarcinomas. Mod Pathol. 2004;17:1223–34.
18. Ohshima S, Shimizu Y, Takahama M. Detection of c-Ki-ras gene mutation in paraffin sections of adenocarcinoma and atypical bronchioloalveolar cell hyperplasia of human lung. Virchows Arch. 1994;424:129–34.
19. Nagasaka T, Sasamoto H, Notohara K, Cullings HM, Takeda M, Kimura K, et al. Colorectal cancer with mutation in BRAF, KRAS, and wild-type with respect to both oncogenes showing different patterns of DNA methylation. J Clin Oncol. 2004;22:4584–94.
20. Dietmaier W, Wallinger S, Bocker T, Kullmann F, Fishel R, Ruschoff J. Diagnostic microsatellite instability: definition and correlation with mismatch repair protein expression. Cancer Res. 1997;57:4749–56.
21. Arai T, Takubo K. Clinicopathological and molecular characteristics of gastric and colorectal carcinomas in the elderly. Pathol Int. 2007;57:303–14.
22. Choi J, Nam SK, Park DJ, Kim HW, Kim HH, Kim WH, et al. Correlation between microsatellite instability-high phenotype and occult lymph node metastasis in gastric carcinoma. APMIS. 2015;123:215–22.
23. Kunisaki C, Akiyama H, Nomura M, Matsuda G, Otsuka Y, Ono HA, et al. Clinicopathological properties of poorly-differentiated adenocarcinoma of the stomach: comparison of solid- and non-solid-types. Anticancer Res. 2006;26:639–46.
24. Japanese Gastric Cancer Association. Japanese classification of gastric carcinoma, 12th ed. Tokyo: Kahahara, 1993 (**in Japanese**).
25. Jiao YF, Sugai T, Habano W, Uesugi N, Takagane A, Nakamura S. Clinicopathological significance of loss of heterozygosity in intestinal- and solid-type gastric carcinomas: a comprehensive study using the crypt isolation technique. Mod Pathol. 2006;19:548–55.
26. Nakajima T, Akiyama Y, Shiraishi J, Arai T, Yanagisawa Y, Ara M, et al. Age-related hypermethylation of the hMLH1 promoter in gastric cancers. Int J Cancer. 2001;94:208–11.
27. Beghelli S, de Manzoni G, Barbi S, Tomezzoli A, Roviello F, Di Gregorio C, et al. Microsatellite instability in gastric cancer is associated with better prognosis in only stage II cancers. Surgery. 2006;139:347–56.
28. Arai T, Esaki Y, Inoshita N, Sawabe M, Kasahara I, Kuroiwa K, et al. Pathologic characteristics of gastric cancer in the elderly: a retrospective study of 994 surgical patients. Gastric Cancer. 2004;7:154–9.
29. van Grieken NC, Aoyama T, Chambers PA, Bottomley D, Ward LC, Inam I, et al. *KRAS* and *BRAF* mutations are rare and related to DNA mismatch repair deficiency in gastric cancer from the East and the West: results from a large international multicentre study. Br J Cancer. 2013;108:1495–501.
30. Fukayama M. Epstein–Barr virus and gastric carcinoma. Pathol Int. 2010;60:337–50.
31. Shinozaki-Ushiku A, Kunita A, Isogai M, Hibiya T, Ushiku T, Takada K, et al. Profiling of virus-encoded microRNAs in

Epstein–Barr virus-associated gastric carcinoma and their roles in gastric carcinogenesis. J Virol. 2015;89:5581–91.
32. Cancer Genome Atlas Research Network. Comprehensive molecular characterization of gastric adenocarcinoma. Nature. 2014;513:202–9.
33. Le DT, Uram JN, Wang H, Bartlett BR, Kemberling H, Eyring AD, et al. PD-1 blockade in tumors with mismatch-repair deficiency. N Engl J Med. 2015;372:2509–20.
34. Colle R, Cohen R, Cochereau D, Duval A, Lascols O, Lopez-Trabada D, et al. Immunotherapy and patients treated for cancer with microsatellite instability. Bull Cancer. 2017;104:42–51.